In Vivo Measurement of T_1 and T_2 Relaxation Times in Awake Pigeon and Rat Brains at 7T

Mehdi Behroozi,[1]* Caroline Chwiesko,[3,4,5] Felix Ströckens,[1] Magdalena Sauvage,[3,4,5] Xavier Helluy,[1,2] Jutta Peterburs,[6] and Onur Güntürkün[1,7]

Purpose: Establishment of regional longitudinal (T_1) and transverse (T_2) relaxation times in awake pigeons and rats at 7T field strength. Regional differences in relaxation times between species and between two different pigeon breeds (homing pigeons and Figurita pigeons) were investigated.
Methods: T_1 and T_2 relaxation times were determined for nine functionally equivalent brain regions in awake pigeons and rats using a multiple spin-echo saturation recovery method with variable repetition time and a multi-slice/multi-echo sequence, respectively. Optimized head fixation and habituation protocols were applied to accustom animals to the scanning conditions and to minimize movement.
Results: The habituation protocol successfully limited movement of the awake animals to a negligible minimum, allowing reliable measurement of T_1 and T_2 values within all regions of interest. Significant differences in relaxation times were found between rats and pigeons but not between different pigeon breeds.
Conclusion: The obtained T_1 and T_2 values for awake pigeons and rats and the optimized habituation protocol will augment future MRI studies with awake animals. The differences in relaxation times observed between species underline the importance of the acquisition of T_1/T_2 values as reference points for specific experiments. **Magn Reson Med 79:1090–1100, 2018. © 2017 International Society for Magnetic Resonance in Medicine.**

Key words: MRI; avian; longitudinal relaxation time; transverse relaxation time

INTRODUCTION

MRI is increasingly used in animals, allowing noninvasive mapping of brain processes in diverse species, which serve as models for neuroscientific questions. The majority of vertebrate models used in neuroscience are rodents (rats and mice), but increasingly bird species such as zebra finches and pigeons also are used. Whereas zebra finches as songbirds are an excellent model for vocal learning (1–3), pigeons typically are used to study mechanisms of learning and memory (4). However, pigeons also are increasingly tested with cognitive tasks assessing functions, such as sequence acquisition (5), equivalence learning (6), categorization (7–9), transitive inference (4), and even orthographic processing (10). A recent study by Levenson et al. (11) even has shown that the capacity of pigeons to visually categorize would make them well suited to identify breast cancer in human tissue samples. In contrast to rodents, some bird species such as corvids additionally demonstrate high cognitive abilities that are equivalent to those of nonhuman primates (12). These include complex social interactions, future planning, tool and meta-tool use, mirror self-recognition, and physical problem solving (13).

Despite this overlap in cognitive performance, birds and mammals differ substantially with regard to structural properties of their brains. In mammals, the telencephalon consists to a large extent of the laminated neocortex. In birds, this laminar architecture is mostly absent and replaced by structures organized in a nuclear fashion (14). Moreover, cellular densities differ substantially between animals, even within a class (15). It is most likely that these differences in structural and cellular organization critically influence the relaxation-time constants of different brain tissues during MRI.

To the best of our knowledge, these relaxation-time constants to date have not been reported for bird brains. Aside from their general value as biophysical properties, these constants are of high practical importance for MRI and functional MRI (fMRI) studies because relaxation times dictate MR signal contrast and signal-to-noise ratio (SNR). Both contrast levels and SNR are required to conclusively separate tissue components and to optimize quantitative sequences in order to obtain other parameters of interest, such as blood perfusion and blood–oxygen-level-dependent (BOLD) parameters. Thus, to obtain reliable results, it is important to quantify relaxation-time constants specifically for the used model species, as well as for different tissue components (16).

Apart from differences in structural brain organization, acquisition of reliable MR data in different species is further complicated by differences in skull structure. Pigeons,

[1]Department of Psychology, Institute of Cognitive Neuroscience, Biopsychology, Ruhr-University Bochum, Bochum, Germany.

[2]Department of Neurophysiology, Faculty of Medicine, Ruhr-University Bochum, Bochum, Germany.

[3]Mercator Research Group, Ruhr-University Bochum, Bochum, Germany.

[4]Leibniz Institute for Neurobiology, Functional Architecture of Memory Department, Magdeburg, Germany.

[5]Faculty of Medicine, Otto von Guericke University Magdeburg, Magdeburg, Germany.

[6]Division of Cognitive Neuroscience, Department of Neurology, Johns Hopkins School of Medicine, Baltimore, Maryland, USA.

[7]Stellenbosch Institute for Advanced Study (STIAS), Wallenberg Research Centre at Stellenbosch University, Stellenbosch, South Africa.

*Correspondence to: Mehdi Behroozi, Faculty of Psychology, Institute of Cognitive Neuroscience, Biopsychology, Ruhr-University Bochum, Universitätsstraße 150, 44780, Bochum, Germany.
E-mail: mehdi.behroozi@ruhr-uni-bochum.de. Twitter: @BehrooziMehdi

for example, possess air cavities in their skulls (17). These cavities cause very strong local magnetic field inhomogeneities, resulting in severe signal loss. As a consequence, gradient echo-planar imaging (EPI) sequences, which are commonly used in fMRI in humans and rodents, cannot be used in pigeons. Instead, fast multiple spin-echo sequences (RARE) in which SNR and signal contrast rely on longitudinal (T_1) and transverse (T_2) relaxation times have been proposed for fMRI in birds (18,19).

The application of functional imaging in awake rodents and birds, which provides several potential advantages over imaging in anesthetized animals (20–24), has introduced even more technical and methodological challenges. Among these challenges, the prevention of movement artifacts by body and head fixation is of utmost importance given that uncontrolled movement can render whole datasets unusable.

The aim of the present study was to address these problems by 1) validating in-house developed fixation protocols to reduce head movement to an absolute minimum for two model species ubiquitously used in scientific research, specifically a mammal (rat, *Rattus norvegicus*), and a bird (pigeon, *Columba livia*); 2) assessing regional T_1 and T_2 relaxation times at 7T in different brain areas in pigeons as compared to rats to check for possible species differences; and 3) also applying said assessment in two different pigeon breeds (homing pigeon and Valencian Figurita) to investigate if relaxation times are also modulated by breed. Typically, homing pigeons and Valencian Figuritas have been bred for different purposes. Homing pigeons have been bred for their navigational skills and flying speed, whereas Figurita pigeons have been bred for a small body size and an angular-shaped head. Therefore, the size and some of the functional properties of the brains differ between these two breeds even though their general neuroanatomy is identical.

METHODS

Sample

Five adult homing pigeons (weight: 330–350 g, 3–4 years old), five adult Figurita pigeons (weight: 170–200 g, 3 years old), and four adult male Long-Evans rats (weight: 400–450 g, 1 year old) were used for the experiments. Animals were housed individually in cages under a 12 h/12 h light/dark schedule and had access to water and food ad libitum. All procedures were carried out in accordance with the guidelines for care and use of animals provided by a National Ethics Committee of the State of North Rhine-Westphalia, Germany.

Head-Holding Apparatus

To prevent motion artifacts, both pigeons and rats were implanted with an MR-compatible plastic pedestal to fixate the animals' heads during MR scanning. For implantation, animals were anesthetized with ketamine/xylazine (70% ketamine, 30% xylazine, 0.075 mL/100 g) and gas anesthesia (only for pigeons: isoflurane (Forane) 100% (volume/volume percent), Mark 5, Medical Developments International, Abbott GmbH and Co KG, Wiesbaden, Germany). The animals' heads were then fixed in a stereotactic apparatus (25). After removing the skin and soft tissues, four to 10 micro pan head screws made of polyether ether ketone were screwed into the skulls in order to provide additional adhesion to the cement. Finally, custom-made plastic pedestals and screws were embedded with dental cement (OMNIDENT, Rodgau, Germany). Following each surgery, analgesic (carprofen (Rimadyl), Zoetis Deutschland GmbH, Berlin, Germany 10 mg/kg) and antibiotic (Baytril, Bayer Vital GmbH, Leverkusen, Germany, 2.5 mg/kg) treatments were administered every 12 hours for at least 3 days.

Habituation Procedure

To reduce the stress associated with head fixation and to minimize body motion artifacts, all animals were habituated to the holding device shown in Figure 1.

For pigeons, an adjustable cloth jacket was used to prevent flapping. The cloth jacket covered the animal's body completely except for the head, neck, and tail. To habituate the animals to being restrained, pigeons were placed in a dark room, while in the jacket, for increasing periods of time over the course of 5 days (15, 30, 60, 90, and 120 min per day). After initial habituation, animals were placed in a custom-made MR-compatible restrainer (Fig. 1) and were fixed via the implanted plastic pedestal. The restrainer was placed in a plastic tube (8-cm diameter) and put into a dark room to simulate the MR scanner bore. Animals took a maximum of 10 days to acclimate to the immobilized condition. The duration of immobilization started at 10 min on the first day and was extended step by step (10, 20, 40, 60, 90, and 120 min per day) until animals were completely habituated to immobilization and head fixation and no longer showed visible stress responses. In the last habituation step, animals were acclimated to the sound produced by the MR scanner (26). For this, pigeons were fixed in place, as described above, and then placed into the actual scanner bore. On the first day, a prepared MRI sequence that was identical to the test sequence was run for 5 min. Scan time was then increased in increments of 5 min until the duration required for the actual experiment (20 min) was reached. Between each increase, animals were given a resting period of 5 min. This protocol was repeated for two consecutive days.

For rats, immobilization was achieved by wrapping the animal in a felt cloth, which was fixed to a plastic carrier with generic hook and loop fasteners. The time of immobilization was extended incrementally over a period of 3 weeks from 3 × 1 min, to 3 × 3 min, 3 × 10 min, 2 × 15 min, and to once 45 min per day. Once animals behaved calmly during 45 minutes of being restrained, they too were habituated to the scanner sound. However, instead of a direct auditory habituation in the scanner, at first only an audio recording of scanner sounds was presented because rats reacted much more strongly to the scanner sounds. Thus, a more gradual habituation process was chosen. After this initial habituation, surgery for head-fixation implantation was performed. After surgery, animals were habituated to the head fixation and the real scanner sounds. To this end, rats were placed in the custom-made rat carrier with their heads lightly immobilized by fixating the head implant
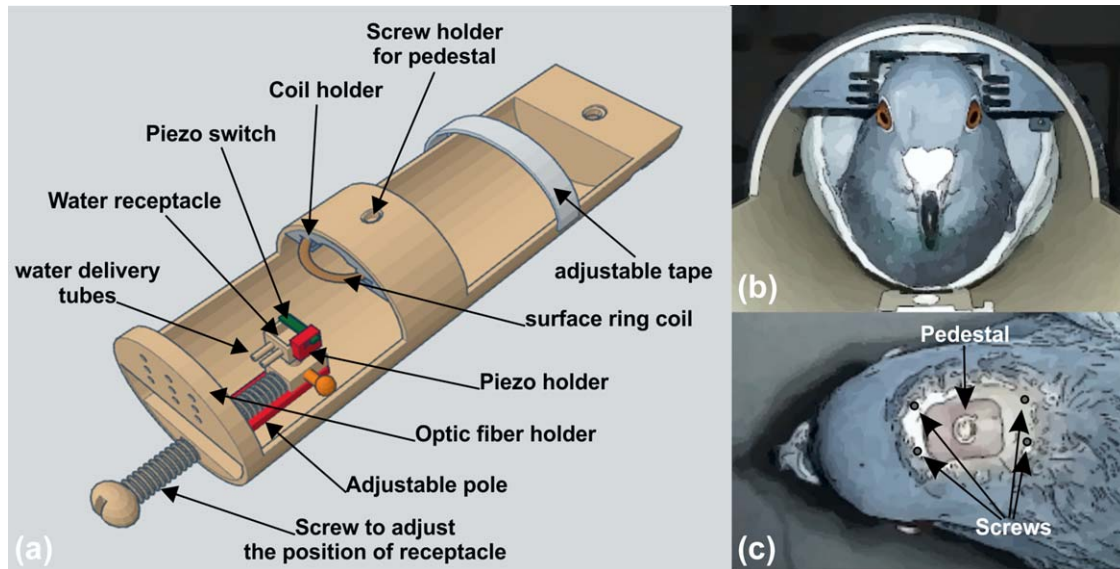
FIG. 1. Schematic drawing of the pigeon restrainer. (**a**) A custom-made MRI-compatible restrainer used in the experiments. Animals were immobilized by a cloth jacket, placed into the restrainer, and fixated via an implanted head pedestal and a plastic screw. The restrainer with the awake animal was then positioned in the middle of the scanner bore with the surface coil positioned directly over the animal's head. A holder for optical fibers, a water receptacle for reinforcement, and a piezo element to detect responses were included in the design to allow for future behavioral experiments in the restrainer. (**b**) Frontal view of the fixated pigeon in the restrainer. (**c**) Location of the head pedestal.

with tape. The rat carrier was then placed next to the MRI scanner for 3 to 5 days to achieve full habituation to the scanner sounds.

MRI Protocols

MRI measurements were acquired with a horizontal bore scanner (BioSpec, 70/30 USR, Bruker, Ettlingen, Germany) using an 80-mm transmit quadrature birdcage resonator and a planar single-loop 20-mm receiver coil from the same vendor. The imaging and shim unit was a Bruker BGA 12s model with 444 mT/m maximal strength. To reduce motion artifacts resulting from body movements, the receiver coil was positioned around the head of the animal and fixed to the animal head-holding system (Fig. 1). MR images were acquired using Bruker ParaVision 5.1 software. During MR scanning, the respiration rate of the animals was continuously monitored using a respiration sensor placed on the breast muscles of the pigeons or on the abdomen of the rats, respectively.

T_1 measurements were acquired using a multiple spin echo saturation recovery method with variable repetition time(TR) (RAREVTR). The following imaging parameters were used: effective echo time (TE) = 53.3 ms; TR array = 0.2, 0.4, 0.7, 1, 1.4, 1.8, 2.4, 3.2, 4.5, 10 s; number of average = 2; RARE factor = 14; matrix size = 256 × 256; field of view (FOV) = 30 × 30 mm^2; resolution = 0.117 × 0.117 mm^2, slice thickness = 1 mm; number of slices = 1 (to avoid interslice signal modulation); read orientation = anterior–posterior. The total acquisition time for T_1 measurements was 13 min 30 s.

For T_2 measurements, the Bruker multi-slice/multi-echo (MSME) sequence was used. Imaging parameters were as follows: TR = 3 s, with an effective spatial bandwidth of 60 kHz; no averaging; number of slices = 1;

number of echoes = 16, with first echo time = 10.73 ms. The geometry was kept identical to the geometry used for T_1 measurements. The total acquisition time for T_2 measurements was 12 min 48 s.

To obtain T_1 and T_2 maps of the pigeon brain, a single slice was positioned directly posterior to the eyes (to avoid eye motion) at A-8.0, according to the atlas of Karten and Hodos (25) to obtain the maximum possible number of regions. To cover as many functionally comparable areas in rats as in pigeons, T_1 and T_2 measurements in rats were taken from two different slices (one coronal at approximately Bregma −3.6 mm, and one sagittal at approximately 3.9 mm from the median plane) in two sequential scanning sessions. To verify the correct location of the coronal slice, one sagittal slice placed exactly in the median plane was recorded (RARE sequence: TE = 15 ms, TR = 4.7 s, RARE factor = 8, FOV = 42.2 × 24.0 mm^2, matrix size = 256 × 160). The coronal slice was then positioned at the posterior end of the thalamus. For verification of the position of the sagittal slice, one coronal slice, placed exactly posterior of the thalamus in the previously obtained median slice, was recorded. The sagittal slice to be used was then placed exactly along the medial boundary of the hippocampus in the said coronal slice. Slice position was verified visually with the rat brain atlas by Paxinos and Watson (27).

As mentioned above, a critical issue in imaging of fully conscious animals is motion artifacts. To evaluate motion parameters for pigeons, MR images were acquired using a T2-weighted RARE with the following parameters: TR = 2 s (acquisition time of each image = 8 s); effective echo time = 60 ms; RARE factor = 16; FOV = 30 × 30 mm^2; matrix size = 64 × 64; number of slice = 5 axial slices; slice thickness = 1 mm; no interslice distance; number of volumes = 100. To evaluate motion parameters

for rats, 10 coronal slices were recorded over a period of 6 minutes using a multi-slice single-shot gradient echo -EPI sequence, TR = 2 s, TE = 17.5 ms, FOV = 21.8×20 mm^2, matrix size = 60×45, slice thickness = 1 mm, interslice distance = 0.2 mm. Data stability was estimated by a 3D ridge body model with a six degrees of freedom affine registration using MCFLIRT (multi-resolution rigid-body coregistration of volume) (28) over a 13-min imaging session.

To investigate the test–retest reliability of T_1 and T_2 measurements, the same animals were scanned twice using the same protocols, with an interval of 6 days between sessions.

Regions of Interest

To determine the precise location of the regions of interest (ROI) in the pigeon brain, a T2-weighted RARE sequence with the following parameters was used to create a whole brain anatomical image: TR = 3 s; effective TE = 75 ms; RARE factor = 16; number of average = 2; matrix size = 256×256; FOV = 30×30 mm^2; resolution = 0.117×0.117m^2; spectral bandwidth = 50 kHz; number of slices = 17 axial slices (centered at the same slice that was used for T_1 and T_2 mapping); slice thickness = 1 mm; no interslice distance. Acquisition time was 3 min 12 s. The whole brain anatomical scan was spatially normalized to the pigeon brain MRI atlas (29) using the functional MRI of the brain (FMRIB) software library toolbox, FMRIB's linear image registration tool (28). The inverted transformation matrix was used to transfer the ROIs from atlas space into an anatomical image. Ten regions, defined based on the pigeon brain MRI atlas (29), were selected bilaterally: entopallium (E); nucleus geniculatus lateralis pars dorsalis (GLd); hyperpallium apicale, including interstitial nucleus of the hyperpallium apicale (HA); hyperpallium intercalatum and hyperpallium dorsal (HI-HD); field L; arcopallium (Arc); striatum (S); amygdala (Am); hippocampus (H); and ventricle (V).

To identify corresponding areas in the rat brain, the recorded coronal and sagittal slices were visually inspected, and the position of ROIs was decided based on the corresponding slices of the Paxinos and Watson rat brain atlas (27). Eleven ROIs, which correspond to the ROIs in the pigeon brain, were selected. In the coronal slice, the following ROIs were selected bilaterally: primary auditory cortex (Au1, corresponds to field L), amygdala (A), primary somatosensory cortex, barrel field (S1BF, corresponds to anterior HI-HD), hippocampus (H), ventricle (V), and corpus callosum (CC, as a white matter structure). In the sagittal slice, the selected ROIs were primary motor cortex (M1, corresponds to arcopallium), primary visual cortex (V1B, corresponds to posterior HA), secondary visual cortex, lateral area (V2L, functionally corresponds to the entopallium, although the entopallium is possibly homologous with regard to its connectivity to medial temporal area (MT/V5)), dorsolateral geniculate nucleus (DLG, corresponds to GLd), and caudate putamen (striatum). For six of the ROIs with a layered structure (S1BF, Au1, M1, V1B, V2L, and H), T_1 and T_2 measurements were taken at three different gray matter levels (superficial, medial, and deep layers). For subsequent analysis, values from these different gray

matter levels were averaged. The CC was selected to obtain a measure of white matter.

Relaxometry Analysis

T_1 and T_2 relaxation-time constants were estimated voxel-wise by nonlinear least square data fitting using the image sequence analysis toolbox of Paravision 5.1 (Bruker BioSpec). T_2 values were estimated using the fit function: $y(t) = A * exp(-t/T_2) + B$, with y(t) as time-dependent signal intensity calculated at various echo times t, A as monoexponential signal intensity prior to any transverse relaxation, and B as the absolute bias. T_1 values were determined by fitting the saturation recovery fit function $y(t) = A(1 - exp(-t/T_1))$, with y(t) as time-dependent signal intensity calculated at the recovery times t, and A as signal intensity after full recovery of the longitudinal magnetization. Next, T_1 and T_2 values within the selected ROIs were averaged for subsequent analysis.

In addition to using the T_2 average from the T_2 maps, we checked the stability of the fit method against low SNR in last echoes by fitting T_2 to the magnitude of the complex signal average of each ROI. Signal-to-noise of the last echo for the signal average was always higher than 10. Statistical testing found no significant differences between the two methods of ROI T_2 estimation ($P > 0.05$).

Estimation of SNR

Signal-to-noise ratio in the images was calculated as signal intensity of a single voxel divided by the standard deviation (SD) of the background noise obtained from a large ROI placed in the image background without any artifacts. The SD of the noise was corrected using the relation $\sigma_{complex} = 1.527\sigma_{magnitude}$ to estimate the SD of the underlying Gaussian distribution of the original complex data.

Statistics

Mean values of T_1 and T_2 time constants for each region were calculated for the different species and breeds. Paired t tests were used to compare T_1 and T_2 time constants within species or breeds, and one-way analysis of variance (ANOVA) was used for between-breed and between-species comparisons, with Bonferroni correction for multiple comparisons. To assess the reliability of measurements, a type of interclass correlation coefficient (ICC) that estimates correlations between two measurements using two-way random effects ANOVA and the absolute argument (30)) was applied on the first and second session dataset. To explore the association between test and retest datasets, Pearson's correlation coefficients were calculated. An ICC close to 1 (maximum value) indicates no within-subject variation, and a value of zero (minimum value) indicates that the data acquired from a single subject at two different time points has large within-subject variations.

RESULTS

Using the habituation protocol described above, both pigeon breeds as well as rats were successfully habituated to the holding device. The custom-made restrainer was
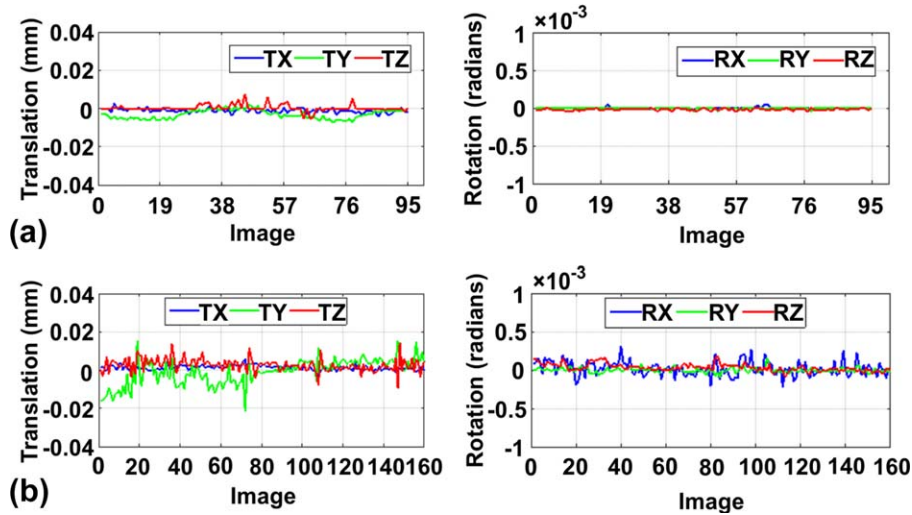
FIG. 2. Estimated motion parameters. (**a**) and (**b**) show translation and rotation parameters estimated by the MCFLIRT toolbox of the FSL 4.0 software for one exemplary pigeon and rat, respectively. Data stability was estimated by a 3D rigid body model with six degrees of freedom for translation and rotation. Blue, green, and red lines in (**a**) and (**b**) correspond to the direction of movement in x-, y-, and z-direction. FSL, functional MRI of the brain (FMRIB) software library; MCFLIRT, multi-resolution rigid-body coregistration of volume.

able to minimize body and head movements. Analysis of data stability demonstrated that all birds and rats were immobile during the scanning process (Fig. 2) (Supporting Fig. S1). Although small movements were visible in the motion parameters, these motions were much smaller than the voxel size (for pigeons: voxel size = 0.46 mm^3, mean motion across all animals in any direction 0.006 ± 0.003 mm (mean ± SD); for rats: voxel size = 0.34 mm^3, mean motion across all animal in any direction 0.031 ± 0.022 mm), and thus were negligible.

Figure 3 shows selected ROIs used to determine T_1 and T_2 relaxation times on a representative series of RARE images from pigeon and rat brains. The selected ROIs corresponded to five main neural systems: visual, auditory, somatosensory, motor, and limbic. T_1 and T_2 relaxation times were also acquired from the ventricle.

Relaxation time values between left and right hemispheres did not show significant differences ($P > 0.05$ for all ROIs; results are not shown). Thus, data were averaged across hemispheres for subsequent analysis. Figures 4a
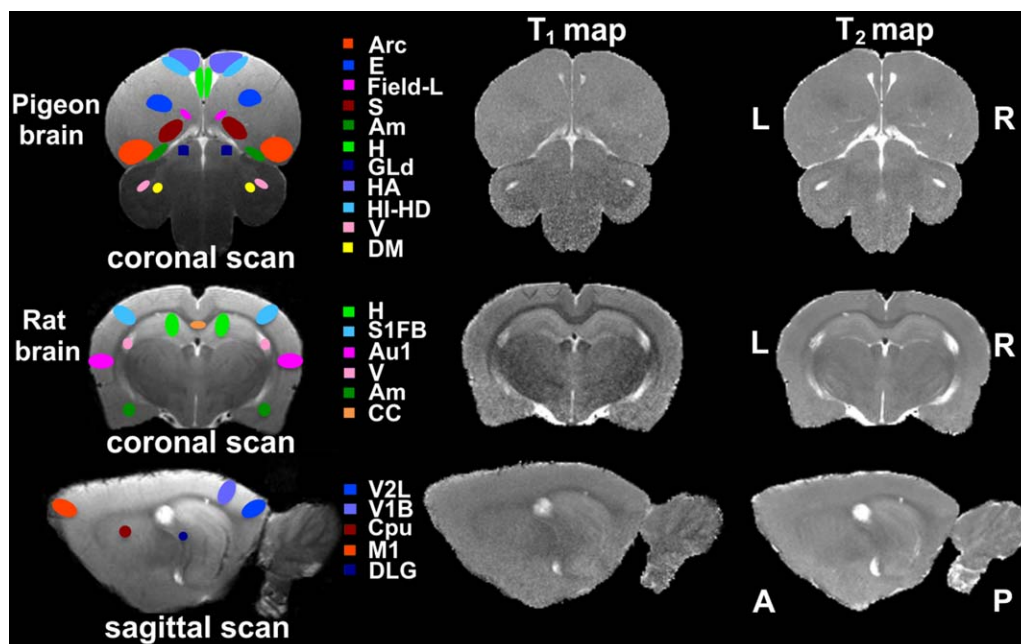

FIG. 3. Image series acquired with the fast multiple spin-echo sequence at 7T from a pigeon (top row, frontal view) and rat brain (middle row, frontal view and bottom row, sagittal view) to indicate relevant regions of interest. T_1 (middle column) and T_2 relaxation maps (right column) for each species are depicted. Note the clear separation of gray and white matter in the rat cortex in the T_1 map, which is mostly absent in the forebrain of the pigeon. A, anterior; Am, amygdala; Arc, arcopallium; Au1, primary auditory cortex; CC, corpus callosum; Cpu, caudate putamen (striatum); DLG, dorsolateral geniculate nucleus; E, entopallium; H, hippocampus; HA, hyperpallium apicale; HI-HD, hyperpallium intercalatum and hyperpallium dorsal; L, left; M1, primary motor cortex; P, posterior; R, right; ROI, region of interest; S, striatum; S1BF, primary somatosensory cortex, barrel field; V, ventricle; V1B, primary visual cortex; V2L, secondary visual cortex, lateral area.
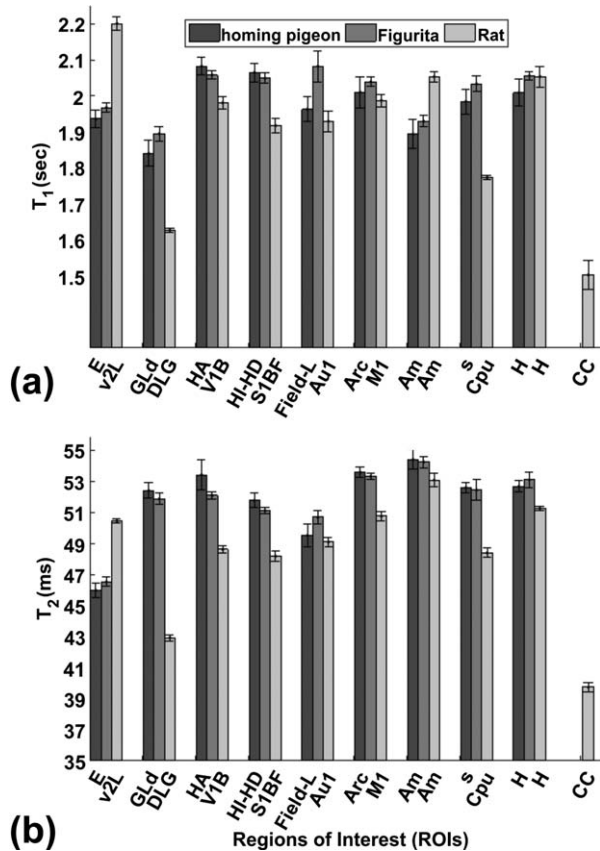
FIG. 4. (**a**) T_1 relaxation times of different ROIs within different species. (**b**) T_2 relaxation times of different ROIs within different species. The plots represent the mean of the relaxation times in each ROI across subjects; error bars represent standard error of mean across subjects.Am, amygdala; Arc, arcopallium; Au1, primary auditory cortex; CC, corpus callosum; Cpu, caudate putamen; DLG, dorsolateral geniculate nucleus; E, entopallium; H, hippocampus; HA, hyperpallium apicale; HI-HD, hyperpallium intercalatum and hyperpallium dorsale; M1, primary motor cortex; S, striatum; S1BF, primary somatosensory cortex, barrel field; V, ventricle; V1B, primary visual cortex; V2L, secondary visual cortex, lateral area.

and 4b summarize the in vivo T_1 and T_2 relaxation times for selected ROIs in pigeons and rats. Standard deviations for each ROI were less than 5%, indicating high consistency of T_1 and T_2 relaxation times within an area. To confirm data quality, an example of T_2 decay, with an echo

spacing of 10.7 ms and T_1 recovery curves, from one of the animals was acquired within the entopallium ROI (Fig. 5).

T_1 and T_2 relaxation times for the different breeds and species were compared by using one-way ANOVAs (Supporting Table S2). For each set of comparable ROIs and for each relaxation time, single one-way ANOVAs were calculated. There were no significant differences in T_1 and T_2 relaxation times between the two pigeon breeds for all analyzed brain regions ($P > 0.0167$, Bonferroni corrected for multiple comparisons). Between rats and pigeons, posthoc analyses revealed that T_1 values differed significantly for all regions, except for the hippocampus, primary auditory areas (field-L and Au1), and primary motor areas (arcopallium and M1) ($P < 0.016$) (see Supporting Table S2). In addition, T_2 values of the analyzed brain regions also differed significantly between rats and pigeons ($P < 0.016$) (see Supporting Table S2), except for primary auditory areas (field-L and Au1) and amygdala. T_1 and T_2 relaxation times for the ventricle did not differ significantly between breeds or species (all $P > 0.05$).

The lowest values for T_1 were found for the GLd in pigeons and the DLG in rats. For T_2, relaxation times were lowest in E in pigeons and in DLG in rats ($P < 0.001$). T_1 and T_2 values for the ventricle ROI were 3.45 ± 0.28 s and 157.2 ± 20.0 ms (mean $\pm$ SD) in pigeons and 3.31 ± 0.32 s and 135.4 ± 38.2 ms (mean $\pm$ SD) in rats. Because differentiation between white and gray matter is absent in birds, we cannot report differences between these for the two pigeon breeds. Average values of T_1 and T_2 for pigeons were 1.98 ± 0.08 s and 51.8 ± 2.6 ms, respectively. In contrast, pure white matter, as measured in the corpus callosum of rats, had the lowest T_1- and T_2-values compared to all other brain regions (Fig. 4). To render the morphological basis of T_1 and T_2 values similar between species, we averaged gray and white matter values for the rats. These averages were 1.94 ± 0.21 s for T_1 and 48.2 ± 4.0 ms for T_2, and no longer differed significantly between pigeons and rats (two sample t test, $P > 0.05$).

To determine test–retest reliability, relaxation times of each animal were acquired a second time in a separate session. Table 1 depicts test–retest reliability results in homing pigeons. Interclass correlation was computed using two-way random effect ANOVA and the absolute argument definition. Interclass correlation results revealed a statistically significant correlation between the two scanning sessions ($P < 0.05$) for all regions. Interclass correlation for T_1 relaxation times

FIG. 5. (**a**) Signal intensity versus different TEs from the pigeon's entopallium at a given repetition time of TR = 3 s (N = 1). (**b**) Signal intensity versus TRs from a pigeon's entopallium at a given echo time of TE = 53.3 ms.TE, echo time; TR, repetition time.
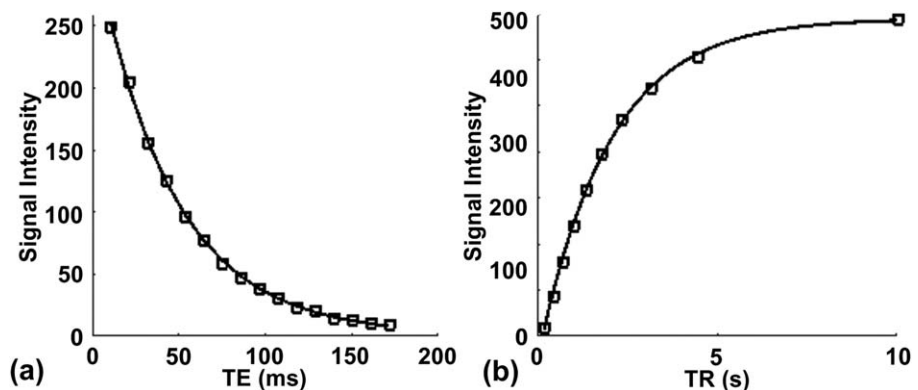
Table 1
Test–Retest Reliability of T_1 and T_2 Relaxation Times for Various Brain Regions in the Awake Homing Pigeon

	T_1 (s)					T_2 (ms)				
Structures	Session 01	Session 02	$ICC_{2,1}$	Paired t Test	r	Session 01	Session 02	$ICC_{2,1}$	Paired t Test	r
Am	1.89 ± 0.09	1.98 ± 0.13	0.82	ns	0.88	54.5 ± 1.4	54.9 ± 1.5	0.97	ns	0.97
Arc	2.01 ± 0.10	2.04 ± 0.15	0.53	ns	0.76	53.6 ± 0.7	53.6 ± 1.1	0.90	ns	0.97
E	1.94 ± 0.06	1.95 ± 0.13	0.68	ns	0.72	46.0 ± 1.0	45.9 ± 1.1	0.88	ns	0.94
Field L	1.96 ± 0.08	1.94 ± 0.11	0.55	ns	0.69	49.5 ± 1.6	49.5 ± 1.6	0.95	ns	0.96
GLd	1.84 ± 0.08	1.80 ± 0.14	0.69	ns	0.76	52.4 ± 1.1	52.3 ± 1.0	0.89	ns	0.89
H	2.01 ± 0.08	2.02 ± 0.14	0.60	ns	0.71	52.7 ± 0.8	52.6 ± 0.8	0.89	ns	0.90
HA	2.08 ± 0.06	2.06 ± 0.13	0.56	ns	0.67	53.4 ± 2.2	53.4 ± 2.0	0.90	ns	0.97
HI-HD	2.07 ± 0.06	2.13 ± 0.13	0.76	ns	0.80	51.8 ± 1.0	51.7 ± 1.3	0.98	ns	0.94
S	1.99 ± 0.08	2.00 ± 0.17	0.88	ns	0.91	52.6 ± 0.8	52.6 ± 0.8	0.93	ns	0.93
V	3.09 ± 0.36	3.09 ± 0.37	0.91	ns	0.99	129.6 ± 16.7	129.5 ± 16.6	0.98	ns	0.98

ICC was calculated using two-way random effects analysis of variance and the absolute argument, $P < 0.05$ in all ROIs for ICCs. T_1 and T_2 means from the same animals were compared using paired t test, where $P > 0.05$ for all ROIs. The values are reported as mean ± standard deviation.
Am, amygdala; Arc, arcopallium E, entopallium; GLd, nucleus geniculatus lateralis pars dorsalis; H, hippocampus; HA, hyperpallium apicale; HI-HD, hyperpallium intercalatum and hyperpallium dorsal; ICC, interclass correlation; ns, not significant; ROI, region of interest; S, striatum; V, ventricle.

ranged from 0.53 to 0.69 for Arc, E, field L, GLd, H, and HA—and from 0.82 to 0.96 for S, Am, HI-HD, and V. Interclass correlations for T_2 relaxation times were bigger than 0.88 for all regions. To control for systematic errors, data from the two sessions were compared using paired t tests. Results showed no significant differences between the two sessions ($P > 0.05$). Test–retest reliability for Figurita pigeons was identical to that of homing pigeons (Supporting Table S1).

DISCUSSION

The present study aimed to establish values for regional T_1 and T_2 relaxation times for several brain regions in awake pigeons and rats at 7.0T field strength. To this end, we first established an optimized habituation and head fixation protocol that allowed for MRI and fMRI in awake animals free of any confounding motion. Relaxation time data were acquired from nine ROIs associated with five main neural systems: visual, somatosensory, auditory, motor, and limbic. Because consistent protocols were used to obtain the MRI data, measurements could be compared between animal species (rats vs. pigeons) as well as between two breeds of pigeons (homing pigeons vs. Figurita pigeons). Results revealed a significant difference between relaxation times in pigeons and rats, whereas no difference was found between the pigeon breeds. These results are of high relevance because they can be used for further optimization of imaging protocols for small awake animals. In the following, we will discuss why imaging in awake animal should be preferred over imaging in anesthetized animals, and what implications the differences in relaxation times between species might have for the present as well as for future fMRI studies.

fMRI in Awake Animals

Immobilization of an animal's head is an important perquisite for obtaining accurate fMRI results. The common procedure to prevent motion of an animal's head during scanning is to use sedation or even deep anesthesia. However, drugs strongly confound MRI results. Most anesthetics significantly affect the proton NMR relaxation of biological tissue. which causes changes in T_1 and T_2 relaxation times (31). Moreover, anesthetics cause changes in the brain state by interacting with cerebral blood flow, cerebral glucose metabolism, and blood oxygenation level, thereby severely affecting the BOLD signal (32). To avoid such distorting effects of anesthesia and to improve generalizability of findings across species, MRI increasingly has been used in awake animals. However, this comes at a cost because it makes head immobilization necessary.

There are two major sources for motion artifacts that can distort the MR signal. The first source is whole head motion caused by the neck muscles. Even minor motion can cause changes in voxel position over the course of a scan and thus distort the signal as a whole. The second source of motion artifacts is motion outside the scanning field of view (33), which can be caused by movements of the eyes, jaw, and lips, or even movements caused by respiration. Although not as severe as whole head motion, these movements can change and obscure the activation map by altering the field homogeneity within the scanned tissue. The custom-made restrainer designed for the present study was able to minimize the first source of motion artifacts in both pigeons and rats (Fig. 1). Thus, our results for both species show that movements during MRI in awake animals can be controlled and prevented: MRI in awake animals is a feasible option and alternative to MRI in anesthetized animals (Fig. 2).

Another important parameter that can substantially affect MRI results, and the BOLD signal in particular, is temperature. During fMRI in anesthetized animals, the body temperature of homeothermic species needs to be stabilized artificially because most anesthetics impair an organism's capability to regulate its body temperature (34). In contrast, MRI in awake animals yields the distinct advantage that the animals can maintain their body temperature independently.

Relaxation Times

Apart from their crucial role in defining MR signal contrast and SNR, reports on NMR relaxation times for

Table 2
In Vivo T_1 and T_2 Relaxation Times for Specific Brain Areas in the Rat at 7T

Structures	T_1 (s)	T_2 (ms)
Am	2.05 ± 0.03	53.1 ± 0.9
Au1	1.93 ± 0.06	49.1 ± 0.6
CC	1.51 ± 0.08	39.8 ± 0.7
Cpu	1.77 ± 0.01	48.4 ± 0.6
DLG	1.63 ± 0.01	42.9 ± 0.4
H	2.05 ± 0.06	51.4 ± 0.6
M1	2.00 ± 0.03	50.7 ± 0.6
S1BF	1.92 ± 0.04	48.2 ± 0.6
V1B	1.98 ± 0.04	48.6 ± 0.5
V2L	2.20 ± 0.04	50.4 ± 0.3

The values are reported as mean ± standard deviation.
Am, amygdala; Au1, primary auditory cortex; CC, corpus callosum; Cpu, caudate putamen; DLG, dorsolateral geniculate nucleus; H, hippocampus; M1, primary motor cortex; S1BF, primary somatosensory cortex, barrel field; V1B, primary visual cortex; V2L, secondary visual cortex, lateral area.

singular brain regions in rodents are surprisingly sparse and, if available, measures were usually obtained from anesthetized animals. In birds, T_2 values were reported for the first time by De Groof et al. (35) in auditory-related regions in anesthetized European starlings. To our knowledge, T_1 values to date have not even been published for anesthetized birds. The reported values for T_2 by De Groof et al. (35) ranged from 27 ± 1 ms in the optic chiasma to 39 ± 3 ms (mean ± SD) in the hyperstriatum ventrale, pars caudalis-robust nucleus of the arcopallium (HVC-RA) tract. Here, we report for the first time the values for T_1 and T_2 relaxation times for awake pigeons and rats (Fig. 4) (Tables 1 and 2) (Supporting Table S1). Regional differences in T_1 and T_2 values were observed between selected ROIs from five main neural systems: visual, somatosensory, auditory, motor, and limbic (Fig. 3), with no differences between hemispheres. Although values between functionally equivalent regions differed between rats and pigeons, there were no differences between the two pigeon breeds (Supporting Table S2).

To allow for comparisons between the present study and previous work, we also have listed T1 and T_2 values obtained from anesthetized rats at 7T, as provided in the literature (Table 3). These values show large variability between different experiments, likely due to differences in hardware, pulse sequence, curve-fitting procedure (22), stimulated echoes, and/or different anesthesia regimes. T_2 values of our rat brain tissue vary between 40 ms and 53 ms and are in the midrange of the values at 7T reported in the literature. Furthermore, they are approximately two times lower than our T_2 measurements in skeletal muscles (T_2 of 23.7 ± 0.6 ms (N = 4)). For comparison with published work, only one reference reports combined brain and muscle T_2 measurements (37). Our T_2 measurements in brain and skeletal muscles reproduce all findings by Crémillieux et al. very well (37). Compared to (37), our T_2 values differ only by 4% in skeletal muscles and are slightly higher in brain tissue, with variations of 7% to 13%, depending on the brain ROIs considered. More research clearly is needed

to systematically characterize the effects of anesthesia on relaxation time, optimally using within-subject designs under controlled conditions. In general, the present study, among the first to report relaxation times for awake animals as well as effective habituation and immobilization protocols, has laid the groundwork for such further investigations.

Notably, the range of T_2 values for different brain regions in European starlings, as reported by De Groof et al. (35), was lower than the range of T_2 values for pigeons in the present study (Supporting Table S3). This difference may be due to the application of very different experimental protocols: thin (400 µm) multiple-slice single-spin echo sequence at two different echo times with animals under anesthesia in (34), versus 1-mm single-slice 16-echo MSME sequence with awake animals in the present study.

In general, the wide range of reported T_2 values in the present study, as well as in previous work, emphasizes the challenges associated with measuring T_2, which mainly are rooted in different experimental difficulties (slice profile, stimulated echoes, and shim) and in the dependence of T_2 on the use of specific sequences and sequence parameters. In the present 7T study, we have used a CPMG sequence with 10.73-ms interpulse interval. Studies in humans and animals have reported that T_2 values measured in brain tissue using CPMG (44) sequences are dependent on the refocusing interval due to dynamic dephasing (45–48) caused by the strong magnetic field gradients created by deoxygenated blood in veins and eventual iron/ferritin deposits. Therefore, it is important to keep in mind that the T_2 values reported in the present study correspond to the so-called apparent T_2, as defined in (47). The reported T_2 values can serve as a valid starting point for optimization of the effective echo time of a given RARE sequence. But in practice and for more tailored results, it may be preferable to remeasure the T_2 value of interest after matching the acquisition parameters related to the CPMG pulse train (in particular, the refocusing interval) in both the MSME pulse sequence used for T_2 mapping and the RARE pulse sequence of interest.

In the present study, specific care was taken to minimize possible confounds that could have overshadowed the between-species comparisons. We used the same hardware and same pulse sequences to obtain T_1 and T_2 relaxation times in all animals. Cross-species comparison of T_1 and T_2 relaxation times showed significant differences between rats and pigeons in T_1 and T_2 values for all regions except for the hippocampus and the auditory and motor regions for T_1, as well as the amygdala and auditory regions for T_2 relaxation times. These differences between species most likely are caused by species-dependent differences in neuro- and cytoarchitecture. The rodent cortex, just like that of all mammals, can be divided into two major components: gray matter and white matter (49). Gray matter mainly is composed of cell bodies as well as neuropil and represents the major information-processing component of the forebrain. In contrast, white matter primarily is made up of bundles of myelinated axons that connect various gray matter regions to each other. In birds, this clear distinction

Table 3

T$_1$ and T$_2$ Relaxation Times in Various Brain Regions of the Anesthetized Rat at 7T, as Reported in the Literature

	References	Anesthesia Regime	ROIs Name	Values	Pulse Sequence Details
T$_2$ (ms)	Massicotte, 2000 (36)	1.5%–2% halothane in a 70:30 mixture of N$_2$O:O$_2$	C CC Cpu	68.8 ± 0.9 61.9 ± 1.2 70.7 ± 1.2	MSME ETL = 8 TR = 1.65 s ES = 20 msec
	Crémillieux, 1998 (37)	ketamine:xylazine (81:11mg/kg)	C CC Cpu CSF H	41.8 ± 1.7 35.8 ± 1.8 42.1 ± 1.5 125.1 ± 9.2 47.9 ± 0.6	MSME ETL = 16 TR = 1 s ES = 8.8 msec
	Liachenko, 2017(38)	1.2%–1.8% isoflurane in O$_2$	Am C Cpu H	61.2 ± 1.4 56.8 ± 0.8 56.4 ± 1.2 58.3 ± 1.1	MSME ETL = 16 TR = 6 s ES = 15 msec
	Gigliucci, 2014 (39)	1.5%–2% isoflurane	CSF H VC	82.8 ± 4.5 52.3 ± 0.4 52.2 ± 0.4	MSME ETL = 12 TR = 2 s ES = 8.1 msec
	Del Bigio, 2011 (40)	1.5%–2% isoflurane in a 70:30 mixture of N$_2$O:O$_2$	C CC Cpu	48.4 ± 0.3 49.2 ± 0.7 50.0 ± 0.3	Spin-Echo ETL = 8 TR = 6 s ES = 20 msec
	Koundal, 2015 (41)	ketamine:xylazine (80:10mg/kg)	CC H	~50 ~56	MSME ETL=11 TR = 6 s ES = 12 msec
	Suleymanova, 2014 (42)	Chloral hydrate (350mg/kg)	Am H	~58 ~60	FSE ETL = 15 ES = 16 msec
T$_1$(s)	Massicotte, 2000 (36)	1.5 to 2% halothane in a 70:30 mixture of N$_2$O:O$_2$	C CC Cpu	1.88 ± 0.02 1.77 ± 0.03 1.75 ± 0.02	TurboFLASH IT = 8 (60–8550 msec) TR = 3.7 msec TE = 2.3 msec
	Barbier, 2005 (43)	5% isoflurane in 30:70 mixture of O$_2$:air	CC Cpu	1.80 ± 0.03 1.64 ± 0.07	FLASH IT = 22 (20–9000 msec) TR = 5.7 msec TE = 3.2 msec
	Del Bigio, 2011 (40)	1.5% –2% isoflurane in a 70:30 mixture of N$_2$O:O$_2$	C CC Cpu	1.78 ± 0.04 1.72 ± 0.08 1.71 ± 0.05	TurboFLASH IT = 8 (246–8738 msec) TR = 3.7 msec TE = 2.3 msec
	Gigliucci, 2014 (39)	1.5–2% isoflurane	H VC	.88 ± 0.02 1.94 ± 0.021	RAREVTR TE = 25.3ms TR = 300–8000 ms

Am, amygdala; C, cortex; CC, corpus callosum; Cpu, caudate putamen (striatum); CSF, cerebrospinal fluid; ES, echo spacing; ETL, echo train length; FSE, fast spin echo; H, hippocampus; IT, inversion times; MSME, multi-slice/multi-echo; ROI, region of interest; TR, repetition time; TE, echo time; VC, visual cortex; RAREVTR, multiple spin echo saturation recovery method with variable repetition time.

between white and gray matter mainly is absent. In addition, the laminar organization of the neocortex, which constitutes major parts of the telencephalon in mammals, is replaced by nuclear-organized structures in pigeons (14). Because gray and white matter differ strongly in terms of relaxation times (50), it is likely that a pure gray matter area in rodents has different relaxation times than a functionally equivalent area in birds in which gray and white matter components are intermingled. Aside from the different neuroarchitecture in mammals and birds, a recent study (15) also demonstrated that avian and mammalian brains differ in neuron density. In all examined avian species, neuron densities were higher than in mammals, with species excelling in cognitive abilities, such as crows and parrots, showing densities twice as high as those in primates. It is likely that these differences also have an impact on relaxation times, thus contributing to the species-dependent differences in T$_1$ and T$_2$ values. Unfortunately, region-specific neuron densities for mammals and rodents, which could explain area-

specific differences in relaxation time between species, have not yet been reported in the literature.

CONCLUSION

The present results confirm that MRI in awake small animals is a feasible alternative to MRI in anesthetized animals, provided that suitable head fixation and habituation protocols are available. We acquired T_1 and T_2 relaxation times for specific brain regions in awake pigeons and rats. We found significant differences in T_1 and T_2 relaxation times between different species but not between two breeds of the same species. We assume that these differences are caused by differences in neuro- and cytoarchitecture between birds and mammals. The reported relaxation times provide comprehensive and quantitative in vivo T_1 and T_2 profiles, and represent a helpful starting point for the optimization of MRI sequences for future MRI studies on awake birds and rodents.

REFERENCES

1. Poirier C, Boumans T, Vellema M, Groof GD, Charlier TD, Verhoye M, Linden AV der, Balthazart J. Own song selectivity in the songbird auditory pathway: suppression by norepinephrine. PLoS One 2011;6:e20131.
2. De Groof G, Poirier C, George I, Hausberger M, Van der Linden A. Functional changes between seasons in the male songbird auditory forebrain. Front Behav Neurosci 2013;7:196.
3. Van der Linden A, Verhoye M, Van Meir V, Tindemans I, Eens M, Absil P, Balthazart J. In vivo manganese-enhanced magnetic resonance imaging reveals connections and functional properties of the songbird vocal control system. Neuroscience 2002;112:467–474.
4. von Fersen L, Delius JD. Long-term retention of many visual patterns by pigeons. Ethology 1989;82:141–155.
5. Scarf D, Colombo M. Representation of serial order in pigeons (Columba livia). J Exp Psychol Anim Behav Process 2010;36:423–429.
6. Friedrich AM, Clement TS, Zentall TR. Functional equivalence in pigeons involving a four-member class. Behav Processes 2004;67:395–403.
7. Yamazaki Y, Aust U, Huber L, Hausmann M, Güntürkün O. Lateralized cognition: asymmetrical and complementary strategies of pigeons during discrimination of the "human concept." Cognition 2007;104:315–344.
8. Watanabe S. Discrimination of painting style and quality: pigeons use different strategies for different tasks. Anim Cogn 2011;14:797.
9. Watanabe S, Sakamoto J, Wakita M. Pigeons' discrimination of paintings by Monet and Picasso. J Exp Anal Behav 1995;63:165–174.
10. Scarf D, Boy K, Reinert AU, Devine J, Güntürkün O, Colombo M. Orthographic processing in pigeons (Columba livia). Proc Natl Acad Sci 2016;113:11272–11276.
11. Levenson RM, Krupinski EA, Navarro VM, Wasserman EA. Pigeons (Columba livia) as trainable observers of pathology and radiology breast cancer images. PLoS One 2015;10:e0141357.
12. Clayton NS, Emery NJ. Avian models for human cognitive neuroscience: a proposal. Neuron 2015;86:1330–1342.

13. Güntürkün O, Bugnyar T. Cognition without cortex. Trends Cogn Sci 2016;20:291–303.
14. Jarvis ED, Güntürkün O, Bruce L, et al. Avian brains and a new understanding of vertebrate brain evolution. Nat Rev Neurosci 2005;6:151–159.
15. Olkowicz S, Kocourek M, Lučan RK, Porteš M, Fitch WT, Herculano-Houzel S, Němec P. Birds have primate-like numbers of neurons in the forebrain. Proc Natl Acad Sci 2016;113:7255–7260.
16. Kimmich R. NMR. Berlin, Heidelberg: Springer Berlin Heidelberg; 1997.
17. Parker WK. VII. On the structure and development of the bird's skull. Trans Linn Soc Lond 2nd Ser Zool 1876;1:99–154.
18. Poirier C, Van der Linden A-M. Spin echo BOLD fMRI on songbirds. Methods Mol Biol 2011;771:569–576.
19. Poirier C, Verhoye M, Boumans T, Van der Linden A. Implementation of spin-echo blood oxygen level-dependent (BOLD) functional MRI in birds. NMR Biomed 2010;23:1027–1032.
20. De Groof G, Jonckers E, Güntürkün O, Denolf P, Van Auderkerke J, Van der Linden A. Functional MRI and functional connectivity of the visual system of awake pigeons. Behav Brain Res 2013;239:43–50.
21. Jonckers E, Güntürkün O, De Groof G, Van der Linden A, Bingman VP. Network structure of functional hippocampal lateralization in birds. Hippocampus 2015;25:1418–1428.
22. van de Ven RCG, Hogers B, van den Maagdenberg AMJM, de Groot HJM, Ferrari MD, Frants RR, Poelmann RE, van der Weerd L, Kiihne SR. T1 relaxation in in vivo mouse brain at ultra-high field. Magn Reson Med 2007;58:390–395.
23. Kara F, Chen F, Ronen I, de Groot HJM, Matysik J, Alia A. In vivo measurement of transverse relaxation time in the mouse brain at 17.6 T. Magn Reson Med 2013;70:985–993.
24. Jonckers E, Van Audekerke J, De Visscher G, Van der Linden A, Verhoye M. Functional connectivity fMRI of the rodent brain: comparison of functional connectivity networks in rat and mouse. PLoS One 2011;6:e18876.
25. Karten HJ, Hodos W. Stereotaxic Atlas of the Brain of the Pigeon (Columba livia). Baltimore: The Johns Hopkins University Press;1967.
26. Hurwitz R, Lane SR, Bell RA, Brant-Zawadzki MN. Acoustic analysis of gradient-coil noise in MR imaging. Radiology 1989;173:545–548.
27. Paxinos G, Watson C. The Rat Brain in Stereotaxic Coordinates. San Diego, CA: Academic Press; 1998.
28. Jenkinson M, Bannister P, Brady M, Smith S. Improved optimization for the robust and accurate linear registration and motion correction of brain images. Neuroimage 2002;17:825–841.
29. Güntürkün O, Verhoye M, De Groof G, Van der Linden A. A 3-dimensional digital atlas of the ascending sensory and the descending motor systems in the pigeon brain. Brain Struct Funct 2013;218:269–281.
30. McGraw KO, Wong SP. Forming inferences about some intraclass correlation coefficients. Psychol Methods 1996;1:30–46.
31. #Karlik SJ, Fuller J, Gelb AW. Anesthetics change tissue proton NMR relaxation. Acta Radiol Suppl 1986;369:500–502.
32. Heinke W, Koelsch S. The effects of anesthetics on brain activity and cognitive function. Curr Opin Anaesthesiol 2005;18:625–631.
33. Yetkin FZ, Haughton VM, Cox RW, Hyde J, Birn RM, Wong EC, Prost R. Effect of motion outside the field of view on functional MR. Am J Neuroradiol 1996;17:1005–1009.
34. Bicego KC, Barros RCH, Branco LGS. Physiology of temperature regulation: comparative aspects. Comp Biochem Physiol A Mol Integr Physiol 2007;147:616–639.
35. De Groof G, Verhoye M, Van Meir V, Balthazart J, Van der Linden A. Seasonal rewiring of the songbird brain: an in vivo MRI study. Eur J Neurosci 2008;28:2475–2485.
36. Massicotte EM, Buist R, Del Bigio MR. Altered diffusion and perfusion in hydrocephalic rat brain: a magnetic resonance imaging analysis. J Neurosurg 2000;92:442–447.
37. Crémillieux Y, Ding S, Dunn JF. High-resolution in vivo measurements of transverse relaxation times in rats at 7 Tesla. Magn Reson Med 1998;39:285–290.
38. Liachenko S, Ramu J. Quantification and reproducibility assessment of the regional brain T2 relaxation in naïve rats at 7T. J Magn Reson Imaging 2017;45:700–709.
39. Gigliucci V, Gormley S, Gibney S, Rouine J, Kerskens C, Connor TJ, Harkin A. Characterisation of the antidepressant properties of nitric oxide synthase inhibitors in the olfactory bulbectomised rat model of depression. Eur Neuropsychopharmacol 2014;24:1349–1361.

40. Del Bigio MR, Slobodian I, Schellenberg AE, Buist RJ, Kemp-Buors TL. Magnetic resonance imaging indicators of blood-brain barrier and brain water changes in young rats with kaolin-induced hydrocephalus. Fluids Barriers CNS 2011;8:22.

41. Koundal S, Gandhi S, Kaur T, Trivedi R, Khushu S. Investigation of prolonged hypobaric hypoxia-induced change in rat brain using T2 relaxometry and diffusion tensor imaging at 7T. Neuroscience 2015; 289:106–113.

42. Suleymanova E, Gulyaev M, Chepurnova N. Ginseng extract attenuates early MRI changes after status epilepticus and decreases subsequent reduction of hippocampal volume in the rat brain. Epilepsy Res 2014;108:223–231.

43. Barbier EL, Liu L, Grillon E, Payen J-F, Lebas J-F, Segebarth C, Rémy C. Focal brain ischemia in rat: acute changes in brain tissue T1 reflect acute increase in brain tissue water content. NMR Biomed 2005;18: 499–506.

44. Carr HY, Purcell EM. Effects of Diffusion on free precession in nuclear magnetic resonance experiments. Phys Rev 1954;94:630–638.

45. Vymazal J, Brooks RA, Baumgarner C, Tran V, Katz D, Bulte JWM, Bauminger ER, Chiro GD. The relation between brain iron and NMR relaxation times: an in vitro study. Magn Reson Med 1996;35:56–61.

46. Brooks RA, Vymazal J, Baumgarner CD, Tran V, Bulte JWM. Comparison of t2 relaxation in blood, brain, and ferritin. J Magn Reson Imaging 1995;5:446–450.

47. Bartha R, Michaeli S, Merkle H, Adriany G, Andersen P, Chen W, Ugurbil K, Garwood M. In vivo 1H2O T2 + measurement in the human occipital lobe at 4T and 7T by Carr-Purcell MRI: detection of microscopic susceptibility contrast. Magn Reson Med 2002;47:742–750.

48. Fischer HW, Rinck PA, van Haverbeke Y, Muller RN. Nuclear relaxation of human brain gray and white matter: analysis of field dependence and implications for MRI. Magn Reson Med 1990;16:317–334.

49. Mai JK, Paxinos G, eds. The Human Nervous System. 3rd ed. San Diego, CA: Academic Press; 2011.

50. Wansapura JP, Holland SK, Dunn RS, Ball WS. NMR relaxation times in the human brain at 3.0 tesla. J Magn Reson Imaging 1999;9: 531–538.

SUPPORTING INFORMATION

Additional supporting information may be found in the online version of this article.

Fig. S1. Motion parameters for individual animals. Each figure shows translation parameters in x, y, and z directions for individual animals. Rotation parameters in any direction were less than 0.01 degree and are not shown.

Table S1. Test-retest reliability the T_1 and T_2 relaxation times in various regions of the awake Figurita brain. Interclass correlation (ICC) was calculated using two-way random effects ANOVA and the absolute argument, $p < 0.05$ in all cases for ICCs. T_1 and T_2 means from the same animals were compared using paired t-test, where $p > 0.05$ for all cases. The values are reported as mean±SD.

Table S2. Results of the statistical post-hoc comparison of T_1 and T_2 relaxation time mean values between homing pigeons (H), figurita pigeons (F), and rats (R). The significance level was Bonferroni-corrected for multiple comparisons ($p < 0.0167$). Significant differences are marked in bold letters. For abbreviations, see Figure 1 and text.

Table S3. Reported T_2 (ms) relaxation times in various regions of the anesthetized starling at 7T as reported by De Groof et al. (35). Animals were anesthetized using ketamine/xylazine mixture. DM=dorsomedial nucleus of the intercollicular complex; HVC = high vocal center; OM=tractus occipito-mesencephalicus; RA=robust nucleus of the arcopallium; LaM=lamina mesopallialis; LMAN=lateral magnocellular nucleus of the anterior nidopallium; LPS=lamina palliosubpallialis; CoA=anterior commissure; CO=optic chiasma; CoP=posterior commissure. The values are reported as mean±SD.